Dynamic Analysis of Stability and Liquefaction in Dams in Unsaturated Soil Mode

Samad Nazari1.*, Mahmoud Hassanlourad2, Elham chavoshi3, Ali Mirzaii 4

Department of Civil Engineering,Isfahan (Khorasgan) Branch, Islamic Azad 2. Mahmoud Hassanlourad, Iran
Assistant profesor, Department of Civil Engineering, Imam Khomeini International University, Qazvin, Iran.University, Isfahan, Iran
Assistant profesor, Department of Soil Science, College of Agriculture,Isfahan (Khorasgan) Branch, Islamic Azad University, Isfahan, Iran
Assistant Professor in Geotechnical Engineering, University of Kashan. Kashan, Iran

Abstract
Liquefaction is one of the destructive phenomenon in soils and terrestrial structures. Liquefaction happens when increase in pore water pressure causes decrease in shear strength in soil. This phenomenon can cause large and unstable subsidence in saturated and unsaturated soil embankments and dams. Regarding that most dams in Iran and the world are earth dams, and are founded on alluvial beds, and liquefaction is probable in these dams, therefore, in order to prevent dam destruction by liquefaction, one needs to consider the mentioned items very carefully. In this study, liquefaction and rupture of earth dams by earthquake in San Fernando as a case is analyzed by GeoStudio Software. The results show how this earthquake causes change in pore water extra pressure, tensions and liquefaction in a wide area of the foundation and core of the dam. This phenomenon causes great changes in forms and ruptures in saturated upstream and unsaturated downstream slopes.

Keywords:
Liquefaction, earth dams, San Fernando earthquake.

1. Introduction

When vibrations or water pressure inside the soil mass causes the soil particles to lose their contact, liquefaction happens. As a result, soil acts as a liquid, is unable to tolerate weight and can flow on very mild slopes. These conditions are usually temporary and often occur because of earthquake in saturated soil embankments or cohesionless soils [1]. When dynamic loads resulting from earthquake occur, loose, sandy, and saturated soil in the region tend to condense and reduce volume. If this soil cannot be drained quickly, because of decrease in permeability coefficient and gradual increase in pore water pressure, effective pressure decreases significantly. In this mode, elasticity module and shear strength of the soil decreases significantly and may result in complete loss of shear strength of the soil [2]. Earth dams are structures directly in contact with water. Proximity with water causes the body and foundation layers of these structures to be saturated. Under such conditions, if the body and foundation of the dam consist of materials with liquefaction potential, dynamic loads on the dam like earthquake on the dam can cause liquefaction and rupture in the dam [3]. In case of liquefaction, serious damage will affect the dam each of which can destroy the dam completely [4-6]. These items can be pointed out:

- Rupture in up and down stream of the dam
- Asymmetric subsidence of dam and as a result, crack in the body
- Decrease in free height of the dam caused by subsidence or change in form of dam crest

Study of quake stability and analysis of liquefaction potential of terrestrial structures, such as dams during earthquakes, are important issues in quake geotechnical engineering [14-7]. Damaging effects of liquefaction caught attention of geotechnical engineers since 1964, after earthquakes in Nigata in Japan and Goodfriday in Alaska [15].

San Fernando dam is an important case study in quake geotechnical engineering and because of its great importance, many researchers have paid attention to it [18-16]. In this study, too, because of the importance of the dam and emergence of liquefaction in it, we attempt to show the modeling method and its analysis in GeoStudio and especially QUAKE/W. Therefore, this important historical phenomenon will be analyzed by GeoStudio Software.

2. Dam Modeling

The mentioned dam San Fernando was hit by an earthquake with the same name and intensity of 6.6 Richter in 1971. The dam is located in the State of California, North of America. The earthquake caused liquefaction in water reservoir equipment known by the name Lower San Fernando and San Fernando reservoir at the northern edge Los Angeles region. Other equipment known by the name

Manuscript received July 5, 2026
Manuscript revised July 20, 2026
https://doi.org/10.22937/IJCSNS.2026.26.7.13

Upper San Fernando also incurred losses which was insignificant.

Figure 1: A bird eye view of San Fernando dam and its reservoir.

In figure 1, once can see a bird-eye view of the whole dam San Fernando reservoir, the lower dam in the left hand picture and the upper dam in the right hand above the picture. Quakes resulting from earth quake caused a fundamental rupture in the upper side of the dam. San Fernando dam is 54 meters high, and with a slope of 2.5h:1v on the sides. The lower side of the body has a drainage channel with a slope of 4h:1v. The dam has a clay core and is directly built on an alluvial bed with a thickness of about 5 meters. The dam and its other body areas and foundation are modeled based on the following figure.

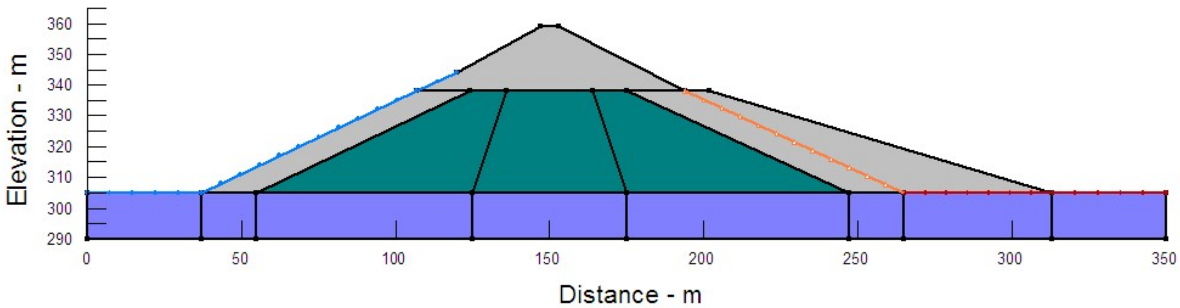

Figure 2: Modeling different parts of the dam in the software

3. Analysis of Seepage in the Dam

Generally, in order to analyze different issues in earth dams, one can consider the soil type and behavior in three modes of saturated, wet, and unsaturated. In the normal mode, a part of the dam body which cuts the water flow is considered saturated soil and the part above 0-pressure line is considered wet or dry. Advantages of this method can be said to be simplicity, reduction on laboratory costs and calculation costs. This is while reaching for more accurate answers requires correct consideration of soil capillary behavior, to which end, one should also calculate the effect of unsaturated soil in the calculations. In these conditions, first the behavior of the soil should be considered unsaturated and with appropriate analysis, saturation effects be considered in the calculations. In such conditions, the soil is saturated gradually in the water flow and the soil above 0-pressure line still has its unsaturated behavior.

In this study, we tried to, assuming unsaturated behavior for the soil, consider capillary effects and gradual seepage correctly. Based on that, we first draw the SWCC chart for body soil and the core of the dam by GeoStudio software. As an instance, the following figure shows SWCC chart for the clay core.

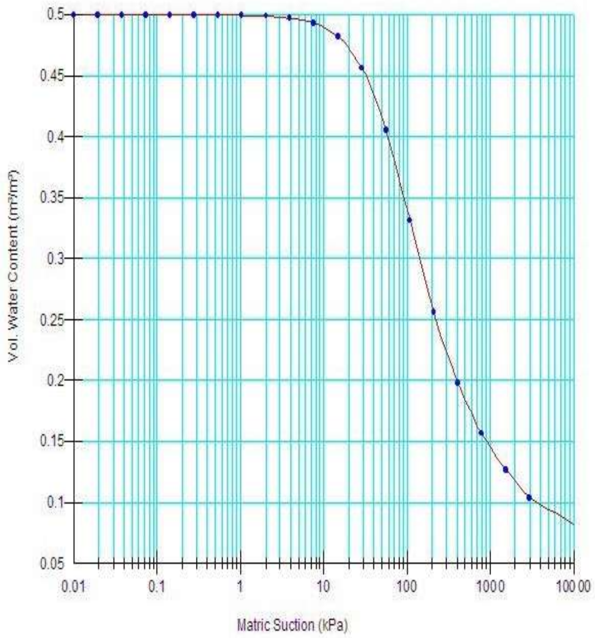

Figure 3: SWCC chart related to soil of dam core

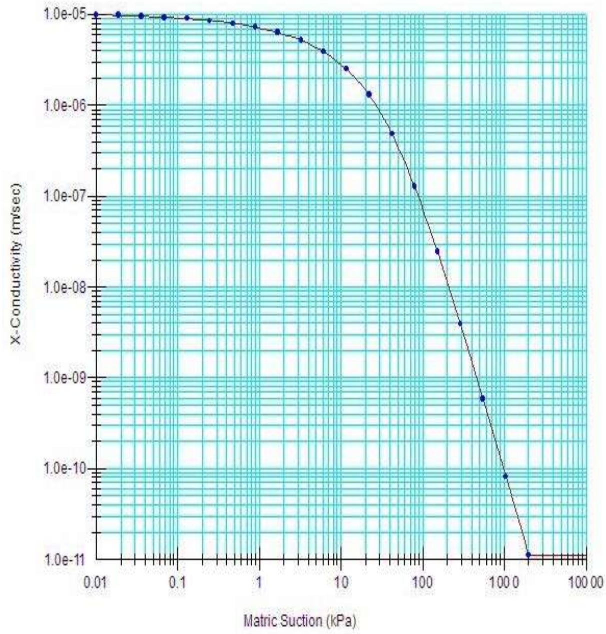

Figure4: permeability of dam body soil based on matric suction

Assuming that in unsaturated soil, permeability of the soil is sensitive to degree of saturation of the soil and is variable, we need to specify the permeability related to each degree of saturation. Based on this, considering SWCC charts, one can provide a chart like figure 4 which is an example for the core, using Geo-Studio software and for permeability, based on matric suction. We should note that permeability charts like figure 4 are obtained based on the Fredlund & Xing approximate method.

Finally, the dam is analyzed for seepage. Figure 5 shows the total head graph for the dam. As one can observe, Blue line represents piezometric line or 0-pressure line. The method for flow and total head distribution is displayed in different colors which is reduced as we move from red color of the head to blue color of the head. Potential reduction lines, too, are almost vertical and flow path lines are displayed almost parallel to piezometric line. In figure 6, too, water flow in the dam body is displayed by black vectors.

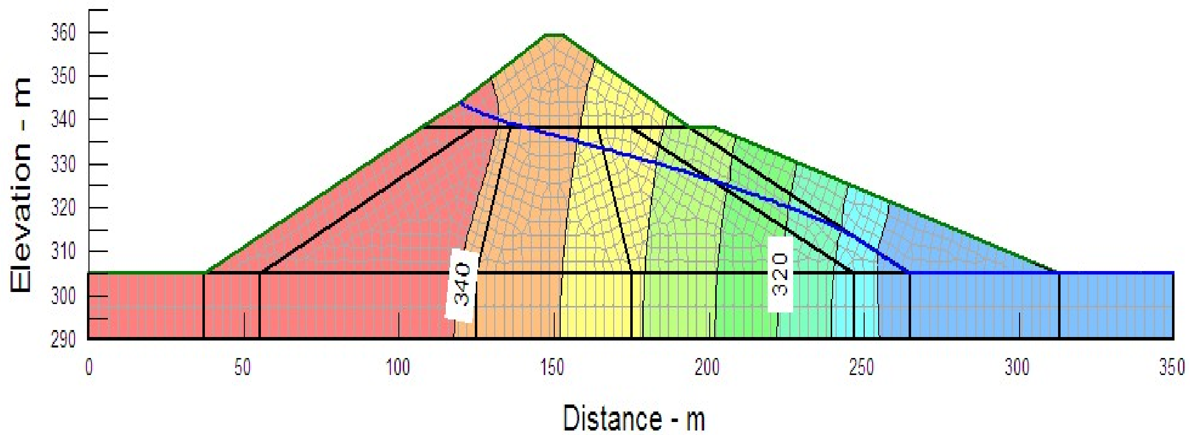

Figure 5: Total head in terrestrial dam body

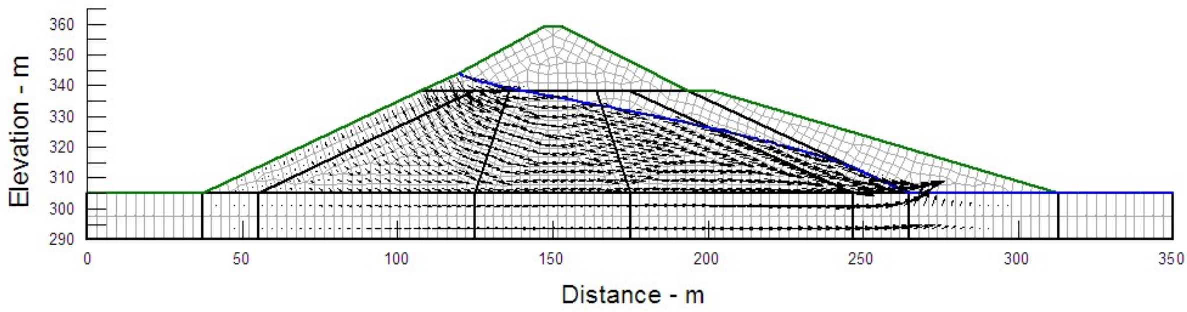

Figure 6: Dam body leakage vector

In figure 7, pore water pressure distribution in different parts of the dam is displayed. Above the 0-pressure line or piezometric line of pore water pressure, negative values for pore water is observed which is because of some analysis in unsaturated mode and unsaturated soil around those areas.

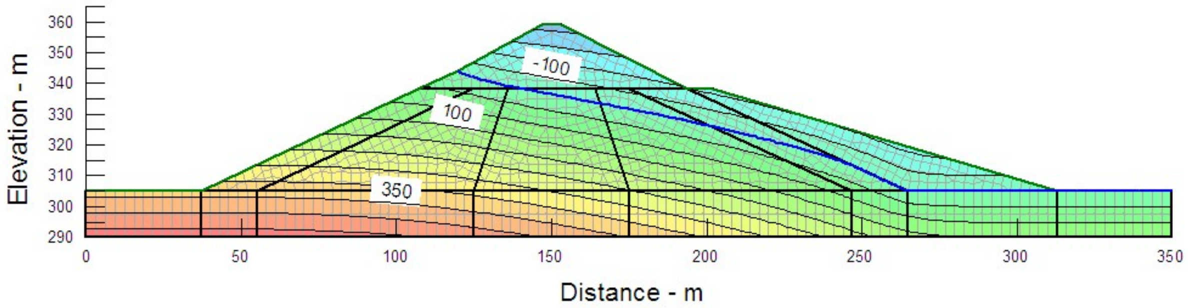

Figure 7: The status of pore water in different layers of the dam

4. Dynamic Analysis

The motion records concerning San Fernando earthquake is registered in different earthquake recording stations. Many previous studies on the dam was conducted using data from Pacomia Dam station 5 kilometers east of San Fernando dam. Motion peak of bed rock in San Fernando site is estimated as 0.6 g and the data values is scaled based on 0.6 g to correspond to this value. The time history registered for this earthquake used in the research is displayed in the figure 8. The beginning and ending quakes are also omitted to reach the 14 seconds time in which the main peaks of the earthquakes occurred.

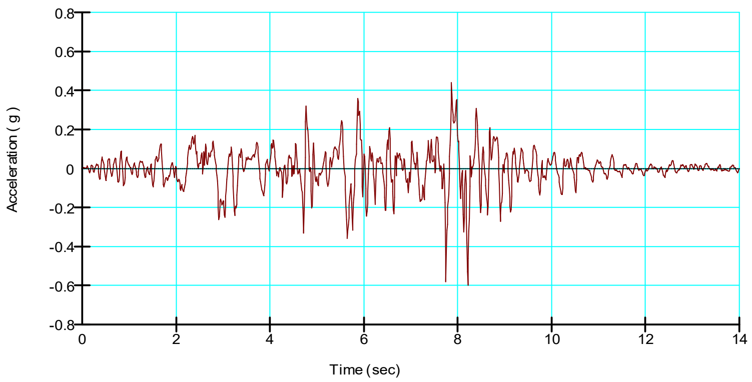

Figure 8: Motion records from earthquake registered by Pacomia Dam station.

Based on the modeling and the recorded motion records concerning the earthquake in 1971, the dam is dynamically analyzed during the earthquake. Figure 9 shows pore water pressure distribution in dam body after the earthquake. Furthermore, in order to better understand the effect of earthquake on dam pore water pressure distribution, the extra pressure for the gathered pore water in the dam is shown in figure 10. As one can see, different parts in the outer layers of upstream and downstream slope layers of the dam experience great extra pore water pressure. The dam, especially at the upper part of downstream slope has experienced the most extra matric suction.

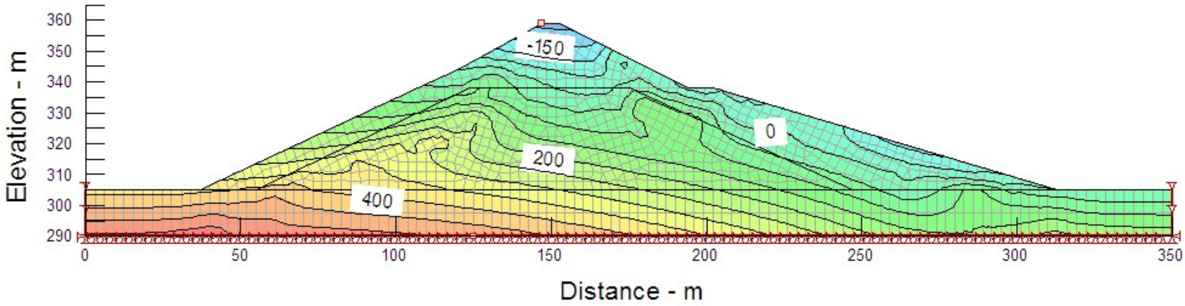

Figure 9: Pore water pressure after earthquake

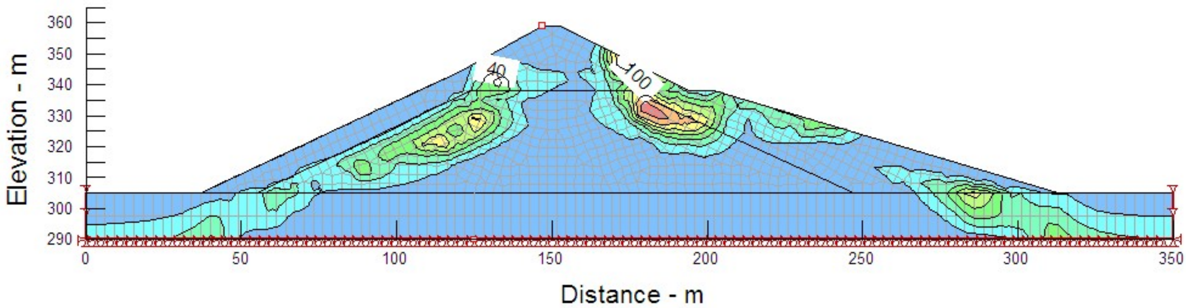

Figure 10: Extra pore water pressure created after earthquake

Corresponding to the dynamical analysis conducted, the total stress and effective stress for the dam is as follows. As one can see in figures 11 and 12, based on the tension expectation from central areas with the most overload, it has the most value compared to areas with the same height. In the lowest areas of the dam center, the total stress reaches more than 1000 KN/m^2 and the effective stress also reaches its maximum values which is about 650 KN/m^2.

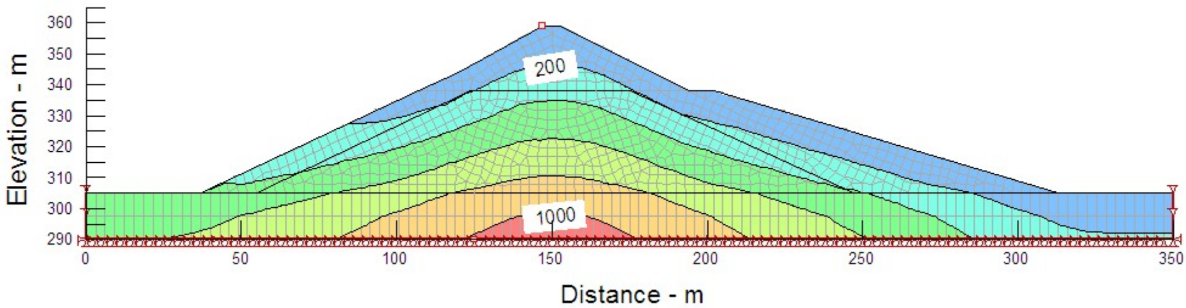

Figure 11: Total stress after earthquake

Manuscript received July 5, 2026
Manuscript revised July 20, 2026
https://doi.org/10.22937/IJCSNS.2026.26.7.13

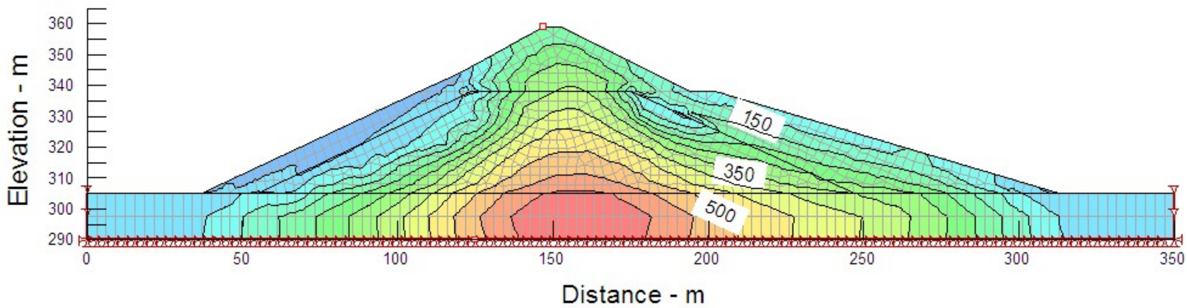

Figure 12: Effective stress after earthquake

For more accurate study and analysis, the total and effective horizontal stress, too, are provided in figures 13 and 14 respectively. As one can observe, the total horizontal stress after the earthquake also has the most value compared to the areas with the same height. After the earthquake, in the bottom areas of the dam center, the total horizontal tension reaches more than 750 KN/m^2 and the effective horizontal stress also reaches its maximum values which is about 350 KN/m^2.

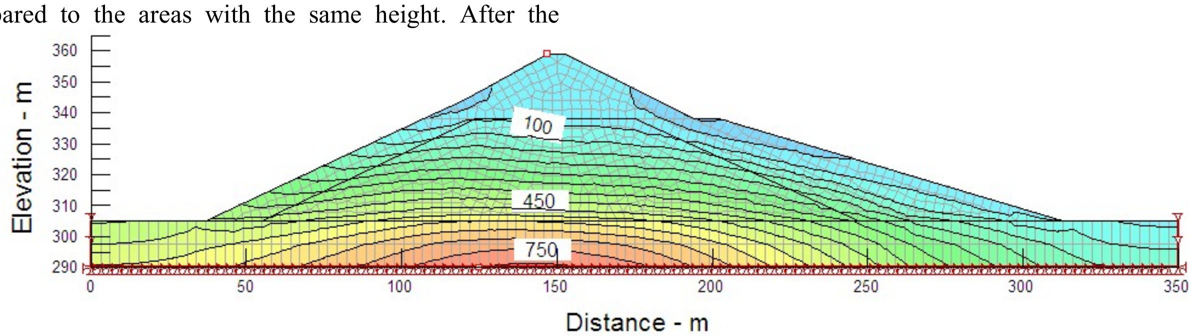

Figure 13: Total horizontal stress after earthquake

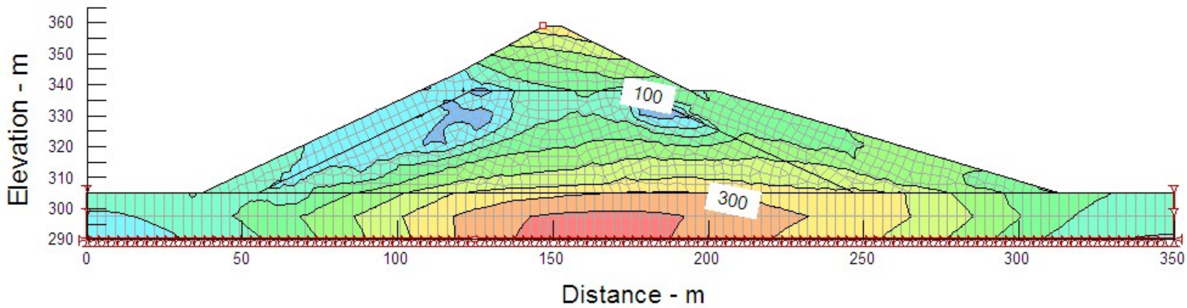

Figure 14: Effective horizontal stress after earthquake

Based on the analysis performed on this dam, the earthquake causes horizontal movements to more than 13 centimeters in the crest. Of course, one should mention that vertical movements have been proportionally less than horizontal movements and reach to at most 5 millimeters in the upstream slopes. Accurate graphs concerning vertical and horizontal movements for this dam are provided in figures 15 and 16 respectively.

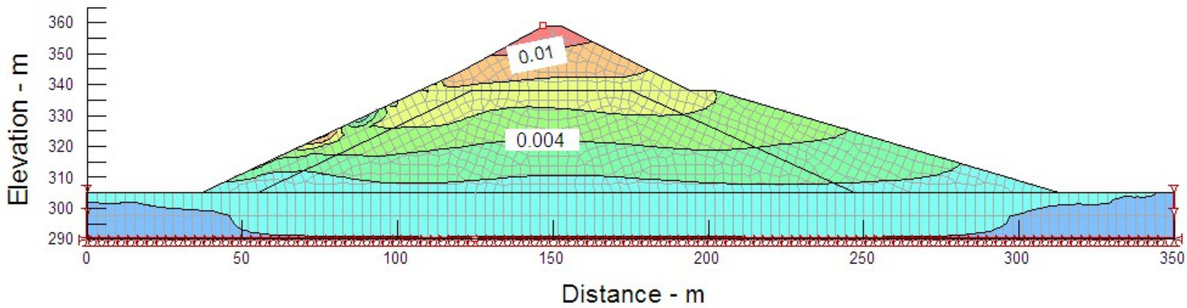

Figure 15: Horizontal movement after earthquake

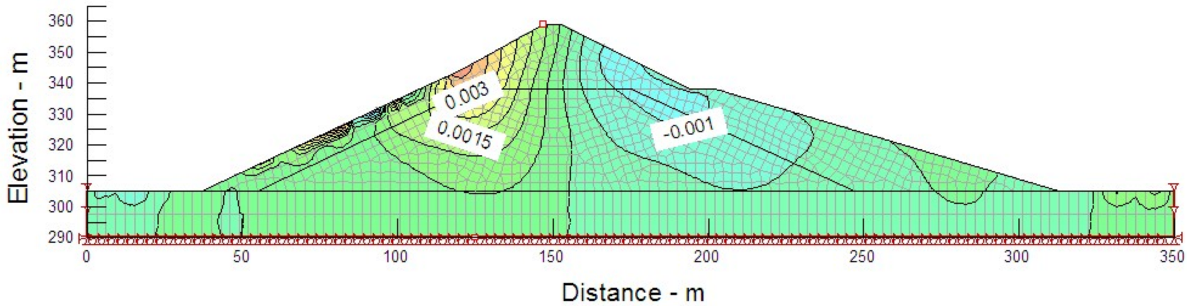

Figure 16: Vertical movement after earthquake

Under normal conditions, the tension status for each point like point B, can experience the conditions of earthquake and increase in pore water pressure till the effective average stress reaches P′ which is the rupture level. Reaching rupture level, the soil resistance conditions can decrease until reaching stable tension status. In case extra increase in pore water pressure causes the effective average stress to decrease, and the effective deviant stress q’ remains constant, until reaching rupture level. This condition is provided in figure 17.

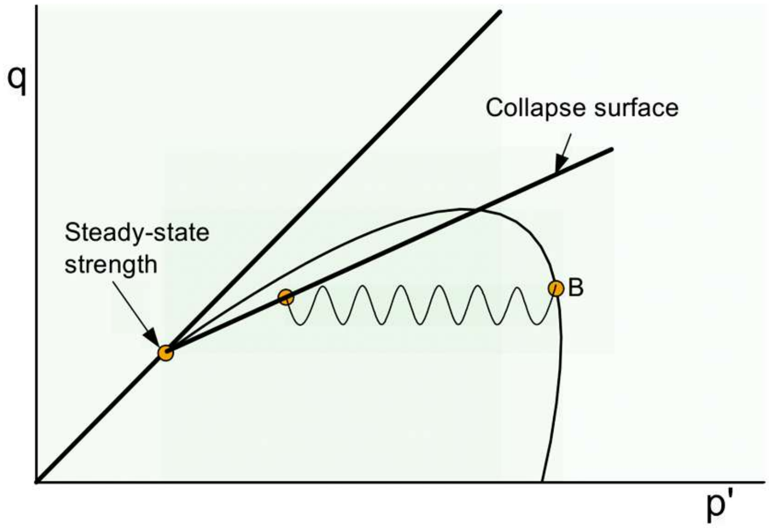

Figure 17: Stress path for loose sand

If soil effective deviator tension in each point in the primary condition is less than resistance tension in stable conditions, increase in extra pressure of pore water and consequently decrease in soil effective average stress, the soil does not turn into liquefaction soil and is transferred to another stress path. Analyzing the stress path in different time steps, one can analyze liquefaction in different elements of the soil and different times. In figure 18, the q/p’ proportion condition is provided in the earth dam body.

Manuscript received July 5, 2026
Manuscript revised July 20, 2026
https://doi.org/10.22937/IJCSNS.2026.26.7.13

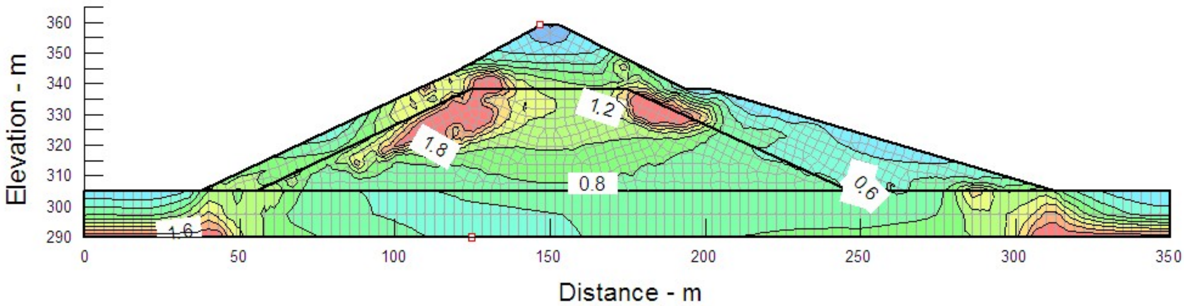

Figure 18: The relativity of dynamic deviator stress to the average stress after earthquake.

Another analyzed issue in this study is Cyclic Stress Ratios (CSR) which is calculated based on the following equation [12].

$$CSR = \left(\frac{\tau_{av}}{\sigma'_{vo}}\right) = 0.65\left(\frac{a_{max}}{g}\right)\left(\frac{\sigma_{vo}}{\sigma'_{vo}}\right)r_d \quad (1)$$

In the above equation, a_{max} is the maximum horizontal acceleration created by earthquake, g is acceleration of gravity, σ_{vo} is the total overload stress, σ'_{vo} is the effective overload stress, and r_d is tension reduction coefficient.

Figure 19 shows the CSR distribution conditions in the dam body after the earthquake.

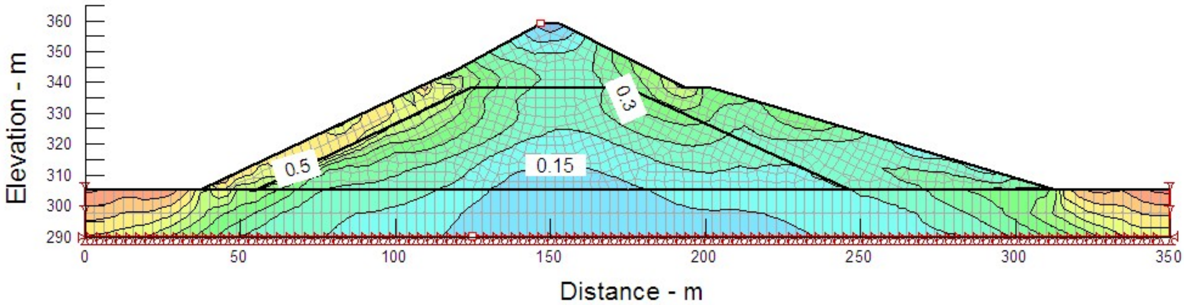

Figure19: The CSR tension condition in the dam body after earthquake

This condition causes liquefaction in many areas. Figure 20 shows liquefied areas after the earthquake. In this figure, yellow areas show regions liquefied because of this earthquake. As one can observe, all the foundation of the dam except for the areas after the hillside of downstream and upstream slopes have become liquefied. Also, core and central areas of the dam have undergone liquefaction.

It seems that the bottom and central parts of the dam have faced liquefaction considering the great overload resulting from upstream and downstream slopes and also impossibility of enough drainage. Furthermore, areas from upstream and downstream which, based on figure 10, have extra pore water pressure, have faced liquefaction.

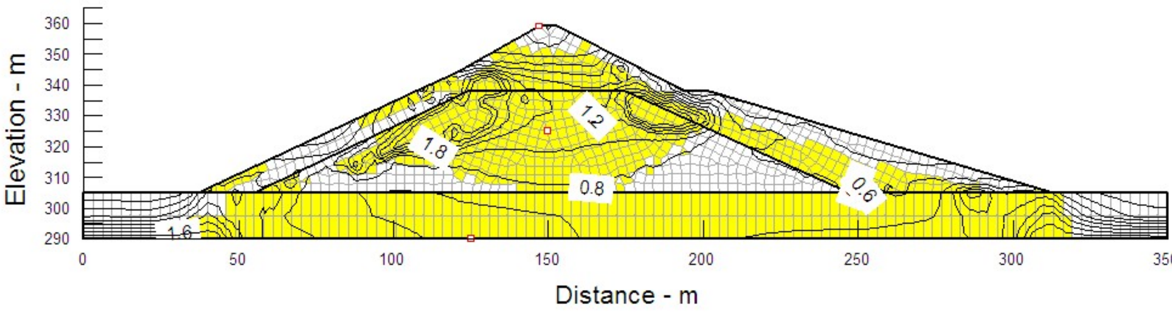

Figure 20: Liquefied areas after earthquake

For instance, for a point of the dam which is located at the core and as a red point, extra pore water pressure is created, horizontal movement, vertical movement, and effective stress changes during the earthquake is studied and analyzed. In figure 21, the extra pore water pressure created at the specified point in the center of the clay core during the earthquake is shown. This extra pressure is 107.70 kPa at the beginning of earthquake, and after that increases linearly and reaches 113.60 kPa in the fourteenth second.

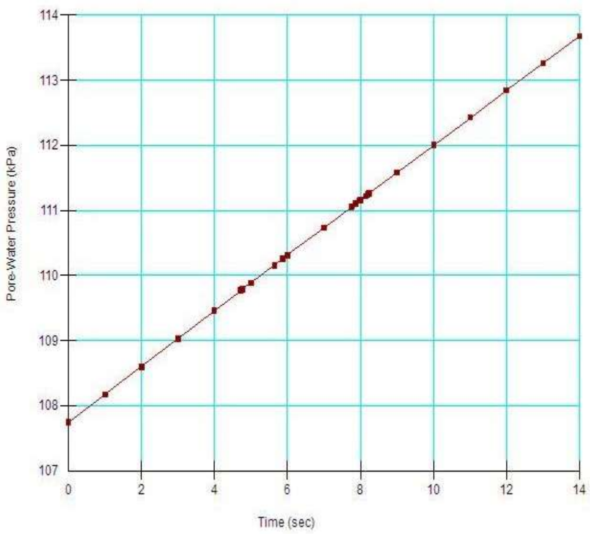

Figure 21: The specified extra pore water pressure in clay core during the earthquake

In figure 22, the horizontal movements created at the specified point in the center of the clay core during the earthquake is provided. One can observe that movements start from zero in the lack of earthquake conditions at zero seconds and after that experiences fluctuations. The maximum limit for horizontal movement occurs at the 3.7 second and is around 10 centimeters, and then experiences location change of 7 centimeters at 4.2 seconds, however, location changes during the 14 seconds of earthquake loading has been averagely around 2 centimeters.

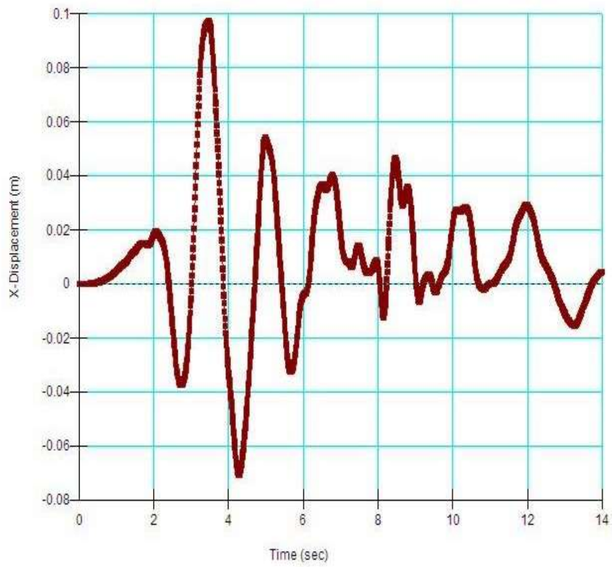

Figure 22: The horizontal movement specified at the clay core

However, the center of clay core has experienced comparatively greater vertical movements than horizontal ones. In figure 23, one can observe vertical movements in the specified points at the center of the clay core during the earthquake. As you can see, vertical movements from zero in lack of earthquake, to the second 2 are insignificant and are almost zero, however, after that, they experience fluctuations. The maximum horizontal movement is about 14 centimeters and happens around 3.9 and 4.2 seconds. Generally, changes in vertical places during 14 seconds of earthquake are averagely about 5 centimeters. We can observe that change in vertical places are significantly more than change in horizontal places of dam core.

Manuscript received July 5, 2026
Manuscript revised July 20, 2026
https://doi.org/10.22937/IJCSNS.2026.26.7.13

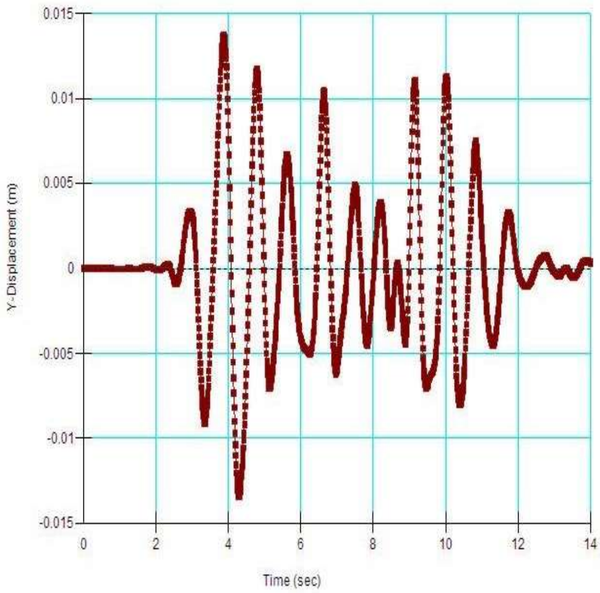

Figure 23: The vertical movement specified at the clay core

Finally, according to figure 25 changes in effective tension in the clay core are analyzed. The results of analysis of effective stress changes during earthquake can be observed on the figure below. The maximum effective stress is at seventh second at 473 kPa and its minimum is at tenth second at 400 kPa.

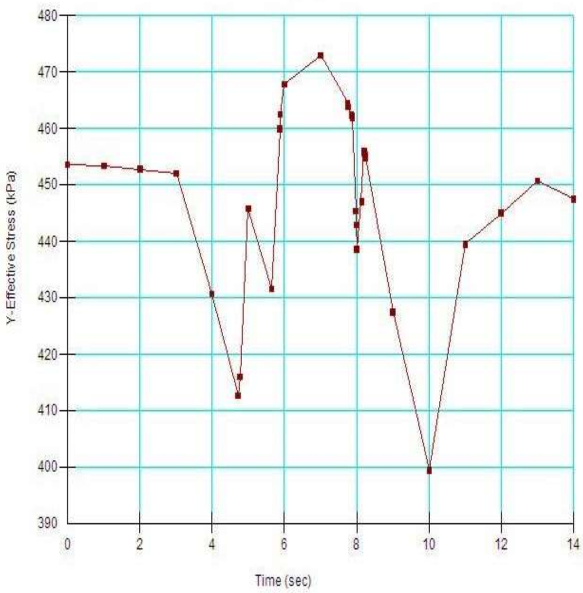

Figure 24: Effective stress changes in the clay core center

In the next step, using the specified tension conditions in each time step, the stable condition of dam sides at downstream and upstream, is analyzed based on finite element method and SLOPE/W sub-software. Changes in the factor of safety in different time steps during the time history of motion recorder at upstream slope is shown in figure 25. We observe that the slope is unstable and at the first second has reached a factor of safety of 0.64 and has ruptured. This slope has experienced factor of safety between fourth and sixth seconds when its maximum movement experienced a factor of safety less than 0.40. Generally, the slope has been very unstable and has had a factor of safety more than 1 in 4.4 seconds.

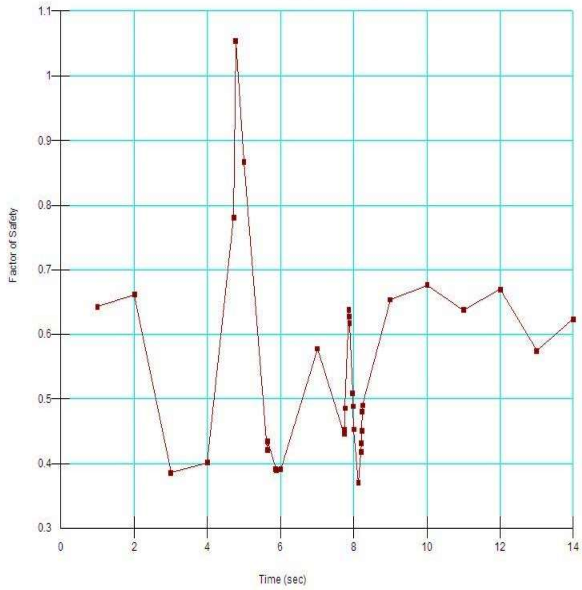

Figure 25: Changes in factor of safety in different time steps for upstream.

Changes in the factor of safety in different time steps during the time history of motion recorder at downstream slope is also studied and shown in figure 26. One can observe that the slope is a little more stable than the upstream slope, however, the slope is not stable and has ruptured during the earthquake. This slope, in the first second, has had a factor of safety of about 1.20 and has been stable. The stability of this slope continues to about 4.5 seconds, however, after that the factor of safety reaches 0.50 and is ruptured. The slope, at about the sixth second when has the most movement, also experienced the lowest factor of safety which was about 0.40. Therefore, the downstream slope is like the upstream slope, however, it ruptures after that. The instability upstream slope is because of its saturation and impossibility of drainage installment.

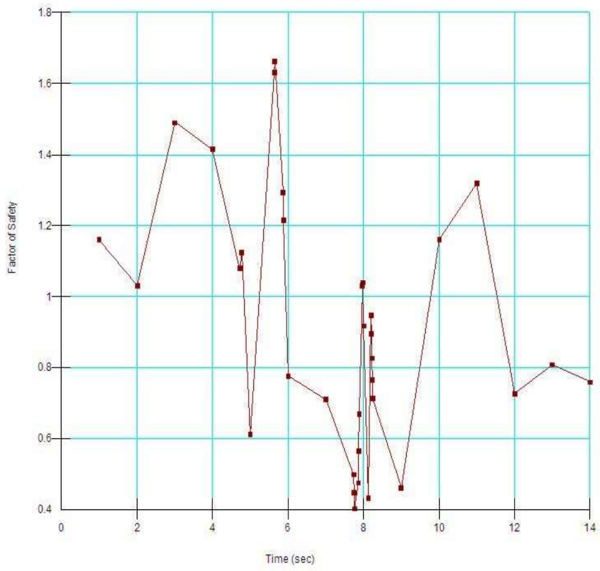

Figure 26: Changes in factor of safety in different time steps for downstream.

5. Changes in Forms Created in the Dam after Liquefaction

In this part, sudden changes in the final form of the dam in the next step after liquefaction is provided. In figure 27, vectors of body form change of the dam after liquefaction are provided. As one can observe, dam crest moves downwards and collapses because of liquefaction. Furthermore, the sides of upstream and downstream have moved sideways. This movement is more observable especially in the upstream side. For better understanding changes in dam form, the zoomed form of the dam after liquefaction is provided in figure 28.

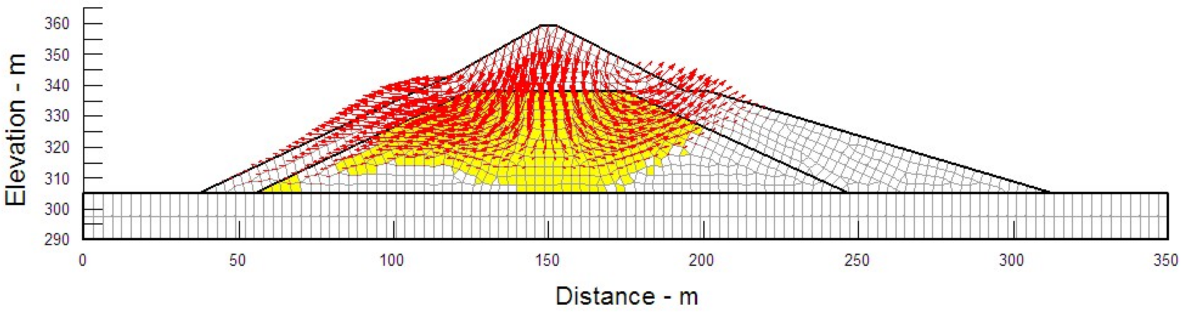

Figure 27: Vectors of body form change after liquefaction

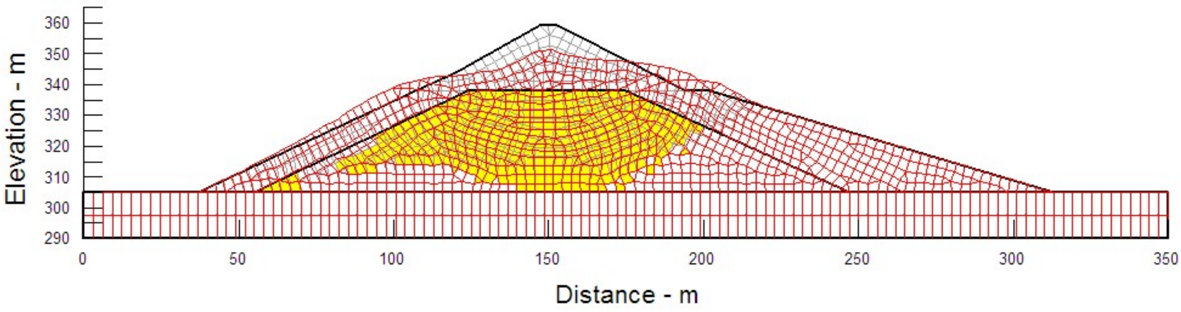

Figure 28: Zoomed form of the dam after liquefaction

6. Conclusion

Generally, in this study, sub-software QUACK/W, SLOPE/W, SEEP/W, and SIGMA/W were used to model and analyze mechanics and liquefaction of the dam under San Fernando earthquake recorder. Therefore, first, the dam was analyzed when full using SEEP/W and after that the conditions of primary tensions were specified in static mode using QUACK/W. After that, using the results of analyses of static tension degree, dynamic analysis was conducted based on San Fernando earthquake and dynamic analysis was conducted in 14 seconds using QUACK/W. In the next step, using the specified tension conditions in each time step, the stable condition of dam sides, is analyzed based on finite element method and SLOPE/W sub-software. The results of these analyses show that both upstream and downstream slopes experience rupture, though instability of downstream slop is lesser. This phenomenon occurs because of unsaturated slope downstream. Finally, the conditions of deformations after liquefaction in the dam body are analyzed using SIGMA/W sub-software. The results of the study show that a significant area of the foundation and core of the dam experience liquefaction.

References

[1] Kramer, S.L., 1996 - "Geotechnical Earthquake Engineering". Prentice Hall. Upper Saddle River.

[2] Seed, H. B. & Idriss, I. M., 1967 - "Analysis of Soil Liquefaction: Niigata Earthquake", Journal of Soil Mechanics & Foundations Division, ASCE, 93(SM3).

[3] Christian H. G., 2001 - "A numerical investigation of the seismic response of the aggregate pier foundation system". Thesis submitted to the Faculty of the Virginia Polytechnic Institute and State University.

[4] Idriss, I.M. and Boulanger, R. W., 2004 - "Semi-empirical procedures for evaluating liquefaction potential during earthquakes" Department of Civil & Environmental Engineering University of California, Davis, Proceedings of the 11th ICSDEE & 3rd ICEGE.

[5] Kayen, R. E., 1992 - "Evaluation of SPT, CPT, and Shear Wave-Based Methods for Liquefaction Potential Assessment using Loma Prieta Data", Proceedings of the 4th Japan-U.S. Workshop on Earthquake Resistant Design of Lifeline Facilities and Countermeasures for Soil Liquefaction, Hamada, M. and O'Rourke, T. D., eds.

[6] Blake, T. F., 1996 - "Liquefaction Resistance of Soils: Summary Report from the 1996 NCEER and 1998 NCEER/NSF Workshops on Evaluation of Liquefaction Resistance of Soils", Journal of Geotechnical and Geo environmental Engineering, ASCE.

[7] Liao, S. S. C. & Whitman, R. V., 1986 - "Catalogue of Liquefaction and Non-liquefaction Occurrences during Earthquakes", Research Report, Department of Civil Engineering, Massachusetts Institute of Technology, Cambridge, Massachusetts.

[8] Rauch, A.F., 1998 - Personal Communication. (as cited in Youd, T. L. 2001 - "Liquefaction Resistance of Soils: Summary Report from the 1996 NCEER and 1998 NCEER/NSF Workshops on Evaluation of Liquefaction Resistance of Soils", Journal of Geotechnical and Geo environmental Engineering, ASCE.

[9] Seed, R. B., 2003 - "Recent advances in soil liquefaction engineering: a unified and consistent framework" 26th Annual ASCE Los Angeles Geotechnical Spring Seminar.

[10] Cetin, K. O., 2000 - "SPT - Based Probabilistic and Deterministic Assessment of Seismic Soil Liquefaction Initiation Hazard", Pacific Earthquake Engineering Research Report No. PEER-2000/05.

[11] Seed, H.B. & Idriss, I.M., 1995 - "Ground Motions and Liquefaction During Earthquakes", publication no. 75-95-2.

[12] Seed, H.B. & Idriss, I.M., 1971 - "Simplified Procedure for Evaluating Soil Liquefaction Potential", Journal of Soil Mechanics & Foundations Division, ASCE, 97(SM9).

[13] Sitharam, T.G., 2004 - "Dynamic properties and liquefaction potential of soils" Department of Civil Engineering, Indian Institute of Science, Bangalore 560 012, India.

[14] Xenaki V.C. & Athanasopoulos G. A., 2003 - Liquefaction resistance of sand-mixtures: an experimental investigation of the effect of fines. Soil Dynamics and Earthquake Engineering, No.23.

[15] Youd, 2001 - "Liquefaction Resistance of Soils: Summary Report from the 1996 NCEER and 1998 NCEER/NSF Workshops on Evaluation of Liquefaction Resistance of Soils", Journal of Geotechnical and Geoenvironmental Engineering, ASCE, 127(10).

[16] Seed, H.B., Lee, K.L., Idriss, I.M. and Makadisi, F.I. 1975. "The Slides in the San Fernando Dams during the Earthquake of February 9, 1971"– ASCE, J of the Geotechnical Engineering Division, GT7, pp. 651-688.

[17] Lee, K.L., Seed, H.B., Idriss, I.M., and Makadisi, F.I. 1975. "Properties of Soil in the San Fernando Hydraulic Fill Dams"– ASCE, J of the Geotechnical Engineering Division, GT8, pp. 801-821.

[18] Seed, H.B., Idriss, I.M., Lee, K.L. and Makadisi, F.I. 1975. "Dynamic Analysis of the Slide in the Lower San Fernando Dam during the Earthquake of February 9, 1971" – ASCE, J of the Geotechnical Engineering Division, GT9, pp. 889-911.